Available online at www.sciencedirect.com
SCIENCE DIRECT®
Nuclear Instruments and Methods in Physics Research A 564 (2006) 339–346
NUCLEAR INSTRUMENTS & METHODS IN PHYSICS RESEARCH Section A
www.elsevier.com/locate/nima

A simple counting technique for measuring mixtures of two pure β-emitting radionuclides

W.M. Van Wyngaardt*, B.R.S. Simpson

CSIR National Metrology Laboratory, 15 Lower Hope Road, Rosebank, Cape Town 7700, South Africa

Received 24 March 2006; accepted 30 April 2006
Available online 16 June 2006

Abstract

A simple counting technique to measure mixtures of two pure β-emitting radionuclides is described. The method is based on elements of two liquid scintillation techniques that are widely used to measure single-radionuclide solutions, namely the triple-to-double coincidence ratio (TDCR) efficiency calculation technique and the CIEMAT/NIST efficiency tracing method. Double- and triple-coincidence count rates, together with the figure-of-merit P determined from an external tracer, are used to extract the component activities of a source. A simulation was used to gauge the effect of counting statistics on the method's ability to extract a mixture composition under normal counting conditions and to validate derived uncertainty formulas based on counting statistics. The method is demonstrated experimentally for various mixture combinations of ^{14}C and ^{63}Ni. It is shown that the accuracy of the technique can be enhanced by improving the determination of the figure-of-merit.

PACS: 23.40.−s; 29.30.Dn; 29.40.Mc; 29.85.+c

Keywords: Pure β-emitting radionuclides; Mixtures; TDCR efficiency calculation; CIEMAT/NIST; Liquid scintillation counting

1. Introduction

Activity measurements of radionuclides decaying by pure β-emission are currently best achieved through liquid scintillation counting. Since β pulse-height spectra are typically broad with continuous energy distributions from zero up to a maximum E_m, liquid scintillation spectra from any combination of different β-emitting radionuclides will overlap. This inherent shape of β spectra together with the low resolution of liquid scintillation detectors make the accurate measurement of mixtures of pure β-emitting radionuclides challenging.

Several methods are available for analyzing the activities of more than one β-emitting radionuclide in the same sample in a relatively short period of time [1]. Disadvantages of these methods are that many of them require the maximum β energies to differ considerably, rely on complicated settings of counting windows and/or on the collection of quench correction curves for the pure components. Recent advances in liquid scintillation analysis have revealed new regionless spectral unfolding and interpolation methods capable of standardizing even mixtures that display strong overlap between spectra [2,3], but complex computer processing as well as quench curves of the pure components are required. A different scheme makes use of rate counting at different times, where a mixed radionuclide source is counted repeatedly for a period of time, usually long compared to the half-life of the short-lived component [4].

This paper reports on a simple alternative approach to measure mixtures of two pure β-emitting radionuclides, which does not rely on complex setting of counting windows, determination of calibration curves for the pure components, spectral analysis or lengthy counting times. The method is based on elements of two liquid scintillation counting techniques that are widely used to measure radionuclide solutions comprising a single pure-β-emitter, namely the triple-to-double coincidence ratio (TDCR) efficiency calculation technique [5,6] and the CIEMAT/

*Corresponding author. Tel.: +27 21 685 7776; fax: +27 21 686 2759.
E-mail address: fvwyngaardt@csir.co.za (W.M. Van Wyngaardt).

0168-9002/$ - see front matter
doi:10.1016/j.nima.2006.04.073

NIST efficiency tracing method [7,8]. Whereas the TDCR technique makes use of the measured triple-to-double coincidence ratio to extract the figure-of-merit of the counting system (and hence the detection efficiency and source activity), measuring a source of unknown mixture composition introduces an additional parameter making the TDCR approach unfeasible. The additional information required to determine the figure-of-merit is obtained from an external tracer standard and this, together with the measured source triple- and double-coincidence count rates, allows the mixture activities to be extracted.

2. Basic principles of the method

To determine the activity of each radionuclide in a source containing a mixture of two known pure β-emitting radionuclides, the source is viewed by a matched three-phototube detection system and both the double-tube coincidence count rate N_d and the triple-tube rate N_t are recorded simultaneously. If the activities of the radionuclides in the mixture are given by N_0 and N_0', respectively, then

$$N_d = N_0\varepsilon_d + N_0'\varepsilon_d' \tag{1}$$

$$N_t = N_0\varepsilon_t + N_0'\varepsilon_t' \tag{2}$$

where $\varepsilon_d, \varepsilon_d', \varepsilon_t$ and ε_t' are the double- and triple-tube detection efficiencies for the respective radionuclides. These efficiencies are determined from theoretical expressions that are functions of the figure-of-merit P that characterises the liquid scintillation counting system [6]. In the method being reported, P is obtained by using a pure β-emitting tracer standard of similar quench to the prepared source, as is done in the CIEMAT/NIST method where ^{3}H is used as the standard.

Eqs. (1) and (2) can be solved for N_0 and N_0' in various ways, the approach adopted here providing insight into the method. Eqs. (1) and (2) are divided by $N_S = N_0 + N_0'$ such that

$$\frac{N_d}{N_S} = r\varepsilon_d + (1-r)\varepsilon_d' \tag{3}$$

and

$$\frac{N_t}{N_S} = r\varepsilon_t + (1-r)\varepsilon_t' \tag{4}$$

where

$$r = \frac{N_0}{N_S} \text{ and } (1-r) = \frac{N_0'}{N_S}. \tag{5}$$

Taking the ratio of Eqs. (3) and (4) to obtain the TDCR indicator N_t/N_d eliminates the unknown quantity N_S. Thus,

$$\frac{N_t}{N_d} = \frac{r\varepsilon_t + (1-r)\varepsilon_t'}{r\varepsilon_d + (1-r)\varepsilon_d'} \tag{6}$$

effectively the weighted triple coincidence efficiency divided by the weighted double coincidence efficiency.

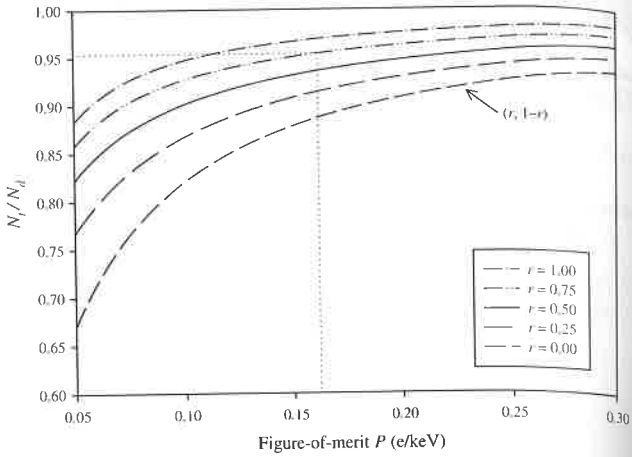

Fig. 1. Curves demonstrating the relationship between N_t/N_d and P for various mixtures of ^{14}C and ^{63}Ni were generated from Eq. (6), where theoretical expressions were used to obtain the counting efficiencies. The fraction of ^{14}C in each mixture is indicated by r and the ^{63}Ni fraction by $(1-r)$. The shapes of the curves will generally be similar for any combination of two pure β-emitting radionuclides.
The dotted lines give an example illustrating the application of the method in practice. If it is assumed that N_t/N_d was measured to be 0.954 and P determined as 0.162 e/keV using an external standard, the intercept of the lines indicates that the measured sample comprised a fractional composition of ^{14}C ($r = 0.75$) and ^{63}Ni ($1 - r = 0.25$). The activities of each component can then be obtained from r as explained in the text.

The concept of the method is demonstrated in Fig. 1. The curves were generated by calculating $\varepsilon_d, \varepsilon_d', \varepsilon_t$ and ε_t' for various figures-of-merit from 0.05 to 0.3 e/keV and for each value of P calculating the corresponding N_t/N_d values from Eq. (6) for five different mixture compositions. In reality, a continuum of lines is possible as r varies from 0 to 1, each curve being referenced by the label $(r,1-r)$.

Measuring a mixed source then entails determining N_t/N_d and P experimentally and the curve corresponding to the intersection of the two values indicates the fractional composition. Once r is known, the required activities N_0 and N_0' can be easily obtained. Mathematically this is achieved by solving for r in terms of N_t/N_d:

$$r = \frac{\varepsilon_t' - (N_t/N_d)\varepsilon_d'}{(N_t/N_d)(\varepsilon_d - \varepsilon_d') - (\varepsilon_t - \varepsilon_t')}. \tag{7}$$

Substitution of the value calculated for r into Eq. (3) or (4) allows the determination of the total source activity N_S whereafter N_0 and N_0' can be calculated from Eq. (5).

However, from a practical point of view, N_0 and N_0' can be obtained more directly by solving Eqs (1) and (2) simultaneously for N_0 and similarly for N_0' to give two solutions that provide the required radionuclide activities from available data

$$N_0 = \frac{N_t\varepsilon_d' - N_d\varepsilon_t'}{\varepsilon_t\varepsilon_d' - \varepsilon_d\varepsilon_t'} \tag{8}$$

$$N_0' = \frac{N_d\varepsilon_t - N_t\varepsilon_d}{\varepsilon_t\varepsilon_d' - \varepsilon_d\varepsilon_t'}. \tag{9}$$

These equations are also particularly useful for the derivation of uncertainty estimators (see Section 3). The results obtained when analysing data with the direct approach are identical to those given by the more lengthy conceptual approach.

3. Simulation

A simulation was performed to gauge the effect of counting statistics on the method's ability to extract a mixture composition under typical counting conditions and to validate derived uncertainty formulas based on counting statistics.

Eleven hypothetical sources containing ^{14}C and/or ^{63}Ni were considered for the simulation. To replicate usual counting conditions, each source was assigned a total activity of 2000 Bq. The ^{14}C content decreased in steps of 200 Bq, from $N_0 = 2000$ Bq in source 1 to 0 Bq in source 11, and the remainder of the activity N'_0 was made up by ^{63}Ni. The simulation mimicked the counting of an actual source by a matched three-phototube detection system, whereby three separate double-tube coincidence counts (D_1, D_2, D_3) and a single triple-tube coincidence count T are collected simultaneously in a time interval t.

The double- and triple-tube detection efficiencies for the respective radionuclides were calculated using a locally modified version of the computer program EFFY 2 [9], imposing that measurements with a similarly quenched tracer standard had given the figure-of-merit of the system to be 0.1621 e/keV.

Exact double- and triple-tube counts (free of statistical variation), D_0 and T_0, were then calculated for each source for a typical counting time of $t = 300$ s, assuming that all three double-coincidence counts were the same

$$D_0 = N_0\varepsilon_d t + N'_0\varepsilon'_d t \tag{10}$$

$$T_0 = N_0\varepsilon_t t + N'_0\varepsilon'_t t. \tag{11}$$

If D is the average of the three pairs of doubles and (X_1, X_2, X_3) are the exclusive double-coincidence counts for each channel, then

$$D_i = X_i + T \quad \text{for} \quad i = 1 \text{ to } 3$$

and

$$D = \frac{3T + X_1 + X_2 + X_3}{3}. \tag{12}$$

Double- and triple-coincidence counts showing realistic variation due to counting statistics were incorporated by varying each independent parameter separately:

$$T = T_0 + f\sqrt{T_0} \tag{13}$$

and

$$D = T_0 + f\sqrt{T_0} + \frac{1}{3}\sum_{i=1}^{3}\left(X_i + g_i\sqrt{X_i}\right) \tag{14}$$

with f and g_i being numbers, essentially between -3 and $+3$, randomly selected from a normal distribution.

For each hypothetical source, double- and triple-coincidence counts (D and T) were simulated for six separate measurements and the ^{14}C and ^{63}Ni activities calculated from Eqs. (8) and (9) after converting the counts to rates. The results were averaged for each source and are given in Table 1 together with the statistical uncertainties. The effect of statistical variation of the double- and triple-coincidence counts on the extracted activities is indicated in more detail in Fig. 2. Normal statistical variation was observed throughout. The simulation clearly demonstrates that counting statistics effects do not impede the method's ability to reliably extract the activities of each component over a wide range of mixture compositions. It also gave pointers as to how many sources and repeat measurements are required in the practical situation to achieve reliable results.

Statistical uncertainties of the extracted activities can be predicted by re-writing Eqs. (8) and (9) in terms of the four independent variables (T, X_1, X_2 and X_3) and applying the uncertainty-propagation formula [10]:

$$\sigma(N_0) = \sqrt{\left(\frac{\varepsilon'_d - \varepsilon'_t}{t(\varepsilon_t\varepsilon'_d - \varepsilon_d\varepsilon'_t)}\right)^2 T + \left(\frac{\varepsilon'_t}{3t(\varepsilon_t\varepsilon'_d - \varepsilon_d\varepsilon'_t)}\right)^2 (X_1 + X_2 + X_3)} \tag{15}$$

$$\sigma(N'_0) = \sqrt{\left(\frac{\varepsilon_d - \varepsilon_t}{t(\varepsilon'_t\varepsilon_d - \varepsilon'_d\varepsilon_t)}\right)^2 T + \left(\frac{\varepsilon_t}{3t(\varepsilon'_t\varepsilon_d - \varepsilon'_d\varepsilon_t)}\right)^2 (X_1 + X_2 + X_3)} \tag{16}$$

where t is the counting time in seconds.

Since the two extracted activities are strongly anti-correlated, an equation for predicting the uncertainty of the sum, $N_S = N_0 + N'_0$, required a determination of the correlation coefficient $r(N_0, N'_0)$. This was calculated in the usual way from the "experimental" variances, $\mathrm{Var}(N_0)$ and $\mathrm{Var}(N'_0)$, and covariance, $\mathrm{Cov}(N_0, N'_0)$ [10], with "experimental" referring to n repeat simulations giving rise to a set of activity values (N_{0i}, N'_{0i}), $i = 1$ to n. Thus,

$$r(N_0, N'_0) = \frac{\mathrm{Cov}(N_0, N'_0)}{\sqrt{\mathrm{Var}(N_0)}\sqrt{\mathrm{Var}(N'_0)}} = \frac{1/(n-1)\sum_{i=1}^{n}(N_{0i} - \bar{N}_0)(N'_{0i} - \bar{N}'_0)}{\sqrt{1/(n-1)\sum_{i=1}^{n}(N_{0i} - \bar{N}_0)^2}\sqrt{1/(n-1)\sum_{i=1}^{n}(N'_{0i} - \bar{N}'_0)^2}} \tag{17}$$

where $\bar{N}_0$ and $\bar{N}'_0$ are the arithmetic means. Once $r(N_0, N'_0)$ is known, the uncertainty of N_S can be predicted by [10,11]

$$\sigma(N_S) = \sqrt{\sigma^2(N_0) + \sigma^2(N'_0) + 2\sigma(N_0)\sigma(N'_0)r(N_0, N'_0)}. \tag{18}$$

The uncertainties predicted by the above-mentioned equations are compared with the statistical uncertainties in Table 1. Good agreement between the two sets of uncertainties indicated consistency within the model.

Table 1
The activities assigned to each hypothetical source, $N_A(^{14}C)$ and $N_A(^{63}Ni)$, are given together with the averaged activities $N_0(^{14}C)$ and $N'_0(^{63}Ni)$ extracted from Eqs. (8) and (9) for each simulated measurement

Source	$N_A(^{14}C)$ Bq	$N_0(^{14}C)$ Bq	$\sigma_m(^{14}C)$ Bq (statistical)	$\sigma_m(^{14}C)$ Bq (predicted)	$N_A(^{63}Ni)$ Bq	$N'_0(^{63}Ni)$ Bq	$\sigma_m(^{63}Ni)$ Bq (statistical)	$\sigma_m(^{63}Ni)$ Bq (predicted)	N_S(Total) Bq	σ_m(Total) Bq (statistical)	σ_m(Total) Bq (predicted)
1	2000.00	2000.47	3.23	1.98	0.00	1.99	2.51	2.09	2002.46	1.48	0.95
2	1800.00	1800.71	1.61	2.01	200.00	197.04	1.01	2.22	1997.75	0.78	1.00
3	1600.00	1599.00	1.94	2.05	400.00	401.55	2.82	2.35	2000.55	0.93	1.06
4	1400.00	1403.69	2.74	2.08	600.00	597.40	3.26	2.47	2001.09	1.63	1.12
5	1200.00	1199.52	2.16	2.11	800.00	800.90	2.33	2.58	2000.43	1.07	1.18
6	1000.00	999.36	3.32	2.15	1000.00	1000.32	4.52	2.69	1999.67	1.89	1.24
7	800.00	799.19	0.84	2.18	1200.00	1200.83	1.67	2.80	2000.02	1.16	1.30
8	600.00	598.36	1.95	2.21	1400.00	1402.41	2.33	2.90	2000.77	1.24	1.36
9	400.00	401.75	1.96	2.24	1600.00	1598.13	1.64	3.00	1999.87	0.77	1.42
10	200.00	200.07	2.02	2.27	1800.00	1797.34	2.72	3.09	1997.41	1.34	1.48
11	0.00	1.93	1.83	2.30	2000.00	1997.88	2.36	3.18	1999.81	1.07	1.53

N_S (Total) is the sum of the extracted individual activities. For each source, the standard deviations of the mean, $\sigma_m(^{14}C)$, $\sigma_m(^{63}Ni)$ and σ_m(Total), were derived from a statistical analysis of the counting data. The corresponding uncertainties predicted by Eqs. (15), (16) and (18), averaged per source and divided by $\sqrt{n}$ (where n = number of repeat measurements), indicated consistency within the model. For the prediction of σ_m(Total), the correlation coefficient $r(N_0(^{14}C), N'_0(^{63}Ni)) = -0.89$, obtained from a statistical analysis of the data, was used.

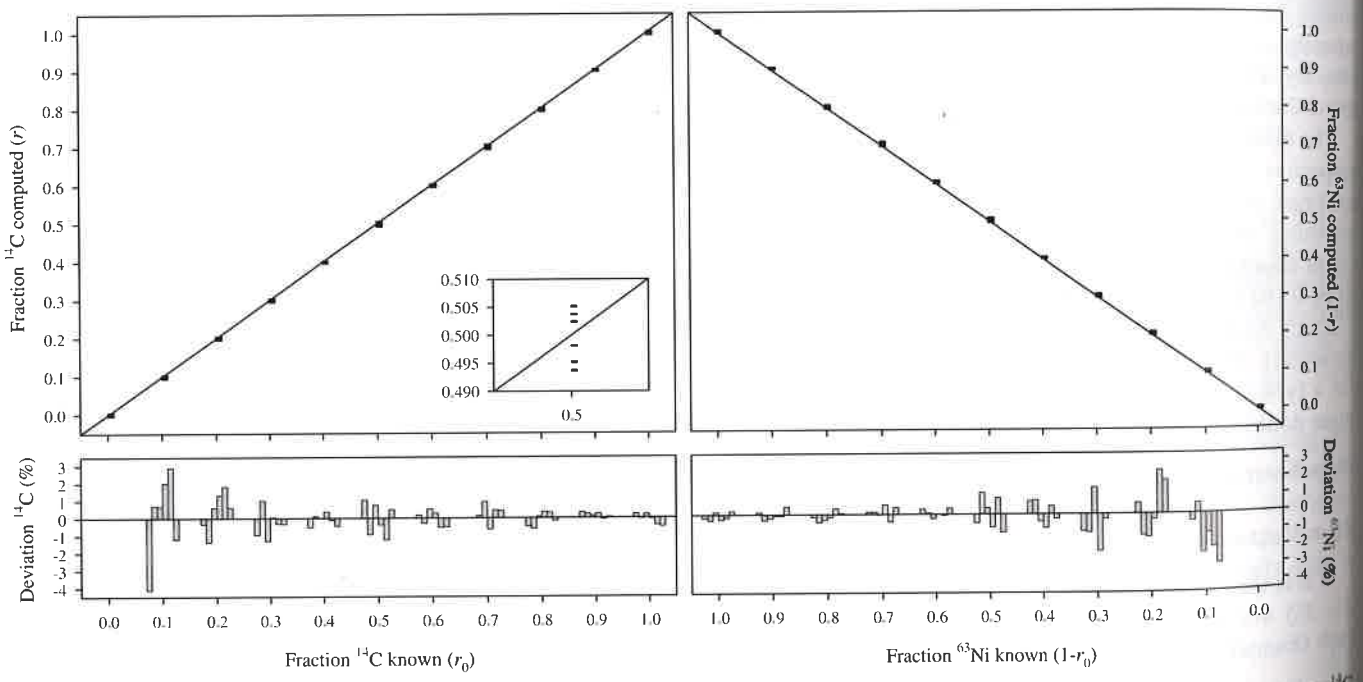

Fig. 2. In the scatter plots, the source compositions computed by the method (r,1−r) are compared with the known compositions (r_0,1−r_0), with the ^{14}C plot on the left-hand side and ^{63}Ni on the right. The diagonal lines indicate the expected ^{14}C and ^{63}Ni fractions, respectively and the black markers are horizontal lines indicating the values extracted from each simulated data set. The inset shows an expanded view of one of the ^{14}C source fractions to emphasize the spread in the extracted values.
The bar diagrams below the scatter plots indicate the percentage deviations (given by $\frac{\text{fraction computed}-\text{fraction known}}{\text{fraction known}} \times 100$) for the ^{14}C and ^{63}Ni fractions, respectively. Normal statistical variation is observed, with the relative deviations increasing as the composition fractions decrease.

4. Experimental

The radionuclides ^{14}C and ^{63}Ni were selected to experimentally demonstrate the feasibility of the technique to resolve mixtures of two pure β-emitting radionuclides. The experimental work was simplified by also using ^{63}Ni as the external tracer standard instead of ^{3}H. In the CIEMAT/NIST method ^{3}H is used to determine the efficiencies of more energetic radionuclides because the propagated uncertainties in the efficiencies are reduced considerably [7]. This reduction in uncertainty will be smaller when ^{63}Ni is used as a tracer due to its higher energy ($E_{max} = 66.945$ keV as opposed to $E_{max} =$ 18.56 keV for ^{3}H [12]), but this will be offset by the smaller uncertainty achievable in the standardization of ^{63}Ni compared to ^{3}H, particularly when using the TDCR

technique. Thus, ^{63}Ni is an acceptable substitution for accurately tracing counting efficiencies.

4.1. Source preparation

Stock solutions of ^{14}C-labelled Na_2CO_3 in an aqueous solution of 486 mg/l Na_2CO_3 and ^{63}Ni-labelled $NiCl_2$ in a solution of 508 mg/l $NiCl_2 \cdot 6H_2O$ in 0.21 M HCl were utilized in the source preparation. In all, 10 sources with different $^{14}C/^{63}Ni$ ratios were prepared by adding accurately weighed aliquots of the stock solutions to 12 ml liquid scintillation cocktail in Wheaton scintillation vials. The scintillator cocktail used was Insta-Gel Plus from Packard Bioscience to which 1.7% (V/V) Carbo-Sorb II from Packard had been added to prevent the loss of ^{14}C due to the reaction of Na_2CO_3 with acid. Sources were labeled M1–M10, with source M1 containing only ^{14}C, source M10 only ^{63}Ni and the sources in-between being the mixed radionuclide sources with the ^{14}C fractions decreasing as the source numbers increased.

The pure ^{63}Ni source M10 was used as the tracer standard for the whole experiment. It was therefore important to prepare the sources so as to match their quench states as well as practically possible. This was done by adding the same total mass of radionuclide solution (varied between 110 and 121 mg) to each source, using the identical liquid scintillation cocktail for all sources (although the pure ^{63}Ni source would not normally require the addition of Carbo-Sorb), and using the same volume of scintillator cocktail for each source. Thus, it was assumed (as a first approximation) that the ^{63}Ni standard could be used to reliably represent the quench state of all the prepared mixed sources and the extracted figure-of-merit P from this source was used throughout.

4.2. Measurements and data analysis

The sources were counted using the NML three-phototube detection system comprising three RCA 8850 high-gain phototubes in a non-symmetrical arrangement [13]. A brief description of the current counting electronics is given in Ref. [14]. The experimental set-up was simple, with only one threshold being set for each channel and counting integrally from just below the single electron peak. Pulses were fed into a locally designed and built coincidence module to provide three pairs of double-coincidence counts and a single triple-coincidence count. The contribution from afterpulsing was monitored and recorded simultaneously with the measured coincidence rates [15]. All counts were corrected for background, deadtime (1.0 μs), coincidence resolving time (0.47 μs) and afterpulsing (up to a maximum of 0.62%, depending on the source and phototube channel). To reduce potential systematic effects due to phototube mismatch, i.e. due to non-reproducible placement of the source relative to the phototubes, not more than three measurements of the same source were made concurrently, with a total of six measurements of 300 s each collected per source. The phototubes were typically matched to within 0.5%.

To determine the expected activity compositions of the prepared sources, the data collected for the two single-radionuclide sources were analysed according to the TDCR efficiency calculation technique [5,6] using a locally modified version of the program EFFY2 [9], where the required ionization quenching function [14] was determined for Insta-Gel Plus ($kB = 0.008$ g/(cm^2 MeV)). The analysis provided the source activities (M10: 3158 ± 16 Bq ^{63}Ni and M1: 2190 ± 11 Bq ^{14}C on 1 February 2005) from which the activity compositions of the mixed-radionuclide sources were determined gravimetrically (Table 2).

4.3. Results

In this experiment, source M10 (^{63}Ni alone) was used as the tracer and TDCR analysis of its counting data provided the figure-of-merit of the system, $P = 0.1621 \pm 0.0017$ e/keV, from which the double- and triple-coincidence detection efficiencies were calculated from the

Table 2
The gravimetric activity composition of each source, $N_G(^{14}C)$, $N_G(^{63}Ni)$ and $N_G(Total)$, are given together with the averaged activities extracted by the method for each source, $N_0(^{14}C)$, $N'_0(^{63}Ni)$ and $N_S(Total)$

Source	$N_G(^{14}C)$ Bq	$N_0(^{14}C)$ Bq	Dev(^{14}C) %	$N_G(^{63}Ni)$ Bq	$N'_0(^{63}Ni)$ Bq	Dev(^{63}Ni) %	N_G(Total) Bq	N_S(Total) Bq	Dev(Total) %	r_0	r
M1	2190.22	2145.05	−2.06	0.00	49.43	—	2190.22	2194.48	0.19	1.0000	0.9775
M2	2041.36	2004.00	−1.83	432.09	474.60	9.84	2473.44	2478.60	0.21	0.8253	0.8085
M3	1791.91	1773.84	−1.01	491.69	504.00	2.50	2283.61	2277.84	−0.25	0.7847	0.7787
M4	1717.52	1712.70	−0.28	851.95	846.39	−0.65	2569.47	2559.09	−0.40	0.6684	0.6693
M5	1338.11	1347.70	0.72	1289.44	1277.80	−0.90	2627.55	2625.50	−0.08	0.5093	0.5133
M6	1008.15	1022.19	1.39	1650.50	1643.97	−0.40	2658.65	2666.16	0.28	0.3792	0.3834
M7	916.93	938.08	2.31	1842.02	1832.76	−0.50	2758.96	2770.84	0.43	0.3323	0.3386
M8	541.96	584.89	7.92	2470.50	2442.03	−1.15	3012.47	3026.93	0.48	0.1799	0.1932
M9	305.39	321.41	5.24	2732.55	2715.86	−0.61	3037.94	3037.26	−0.02	0.1005	0.1058
M10	0.00	−1.97	—	3158.08	3160.78	0.09	3158.08	3158.81	0.02	0.0000	−0.0006

The deviations of the averaged measured activities from the gravimetric compositions are given relative to the radionuclide activities $\left(\%\text{-deviation} = \frac{\text{fraction measured} - \text{fraction prepared}}{\text{fraction prepared}} \times 100\right)$. The ratios r_0 and r indicate the gravimetric and measured activity fractions of ^{14}C.

EFFY2 programme: ^{14}C ($\varepsilon_d = 0.8678$, $\varepsilon_t = 0.8409$) and ^{63}Ni ($\varepsilon_d = 0.5910$, $\varepsilon_t = 0.5242$), where the efficiencies are given in units $s^{-1}\,Bq^{-1}$.

The corrected double- and triple-coincidence counts for each measurement were substituted into Eqs. (8) and (9) together with the above calculated efficiencies to extract the radionuclide activity compositions. The activities thus determined were summed to give the total activity for each measurement. The results, averaged for each source, are given in Table 2 together with the relative deviations. In Fig. 3, the measured activity fractions are compared with the expected values for each individual measurement. The extracted activities of each component compare well with the prepared activities over a wide fractional range, although the deviations display a systematic trend for each radionuclide, changing from positive to negative as the fraction increases.

4.4. Discussion of errors and uncertainties

The errors and uncertainties observed for the extracted activities are most clearly explained with reference to Fig. 1.

(i) *Effect due to counting statistics*: Since radioactive decay is by nature a random process, N_t/N_d will vary from measurement to measurement so that a different $(r,1-r)$ curve is selected each time, giving rise to statistically varying, anti-correlated extracted activities. The uncertainties due to counting statistics can be estimated from Eqs. (15) and (16) and are given in Table 3 for the measurements of the mixed radionuclide sources.

(ii) *Other effects affecting the counts and hence* N_t/N_d: Afterpulsing could only be measured for one of the double coincidence channels at a time and the after-

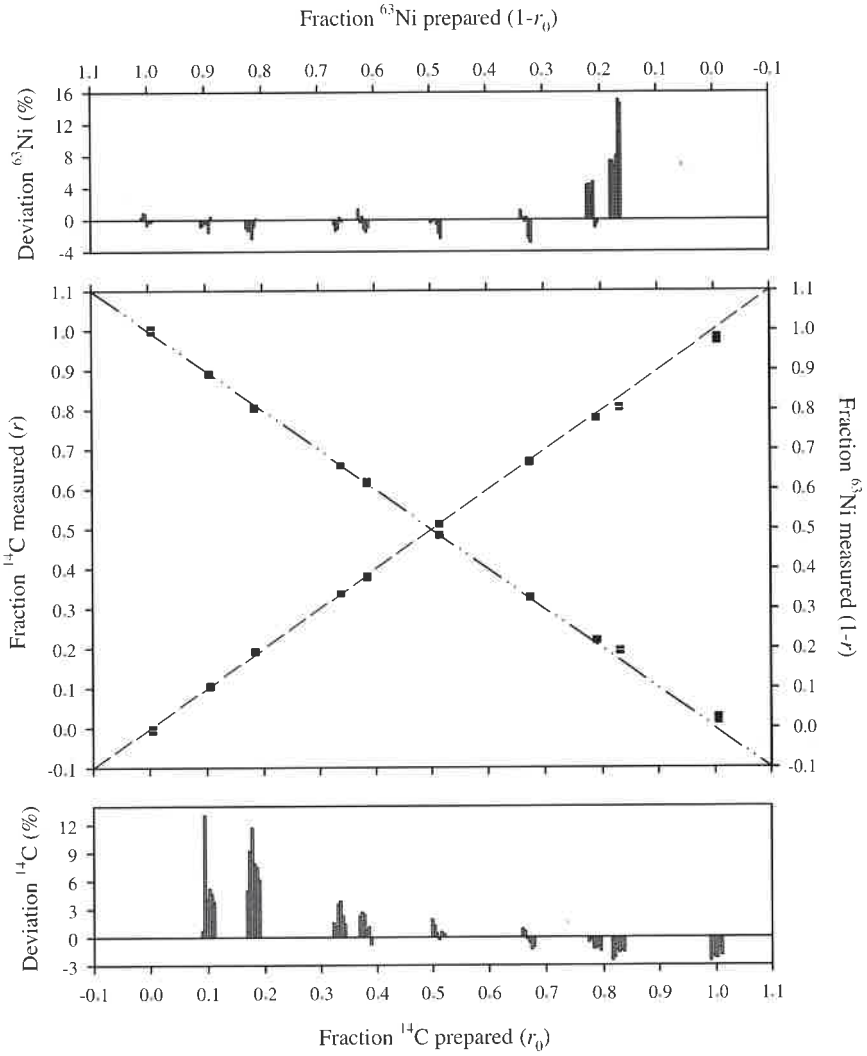

Fig. 3. In the scatter plot, the source compositions extracted by the method $(r,1-r)$ are compared with the gravimetric compositions $(r_0,1-r_0)$. The diagonal lines indicate the expected compositions (^{14}C broken line, ^{63}Ni dash-dot-dot). The markers are horizontal lines indicating ^{63}Ni and ^{14}C compositions calculated by the method for each measurement. The bar diagrams above and below the scatter plot indicate the percentage deviations (given by $\frac{\text{fraction measured}-\text{fraction prepared}}{\text{fraction prepared}} \times 100$) for the ^{63}Ni and ^{14}C components, respectively, for each repeated measurement of a given source. As is expected, the relative deviations increase as the activities decrease.

Table 3
The additional spread in results from repeat measurements of the same source is given by the difference (in quadrature) between the uncertainty contribution due to measured statistical variation and that calculated for counting statistics from Eqs. (15) and (16)

Source	^{14}C			^{63}Ni		
	Measured statistical variation (%)	Counting statistics (%)	Additional statistical spread (%)	Measured statistical variation (%)	Counting statistics (%)	Additional statistical spread (%)
M2	0.19	0.08	0.17	1.44	0.55	1.34
M3	0.19	0.09	0.17	1.05	0.50	0.92
M4	0.37	0.10	0.36	0.68	0.33	0.59
M5	0.31	0.14	0.27	0.40	0.24	0.32
M6	0.54	0.19	0.50	0.45	0.20	0.40
M7	0.46	0.22	0.41	0.28	0.18	0.21
M8	0.88	0.39	0.79	0.34	0.15	0.31
M9	1.60	0.73	1.43	0.27	0.14	0.24

Contributors to this additional spread are uncertainty in the correction for afterpulses, deadtime, coincidence resolving time and background and also phototube mismatch. The uncertainty contributions are given relative to the specific radionuclide activities at 1σ.

pulse correction for each measurement was thus determined from data collected during three separate measurements of the same source. The resultant uncertainty in the N_t/N_d ratio can lead to the selection of an incorrect $(r,1-r)$ curve. This is probably a random effect increasing the spread of measured activities, but it could also be responsible for a systematic trend.

The corrections made for deadtime, coincidence resolving time and background each have a small uncertainty and could thus also affect N_t/N_d, resulting in the selection of a somewhat incorrect curve.

These random effects all contribute to the additional uncertainties given in Table 3.

(iii) Effects due to variation in P:

(a) Non-reproducible placement of a counting vial leads to asymmetry in the phototube efficiencies. This variation in phototube matching leads to an actual net figure-of-merit different from the P value used and the incorrect $(r,1-r)$ curve is selected. This effect probably averages out between repeat placements of the same source giving close to the "true" activity values, but it spreads out the results giving a larger standard deviation. This effect also contributed to the additional uncertainties given in Table 3.

(b) If the value of P used (as given by the tracer standard) does not properly correspond to the actual quench state of the mixture source, the incorrect $(r,1-r)$ curve will be selected, leading to systematically higher or lower extracted activity values. The assumption that the quench states of all sources used in the experiment were the same was not strictly correct. This is demonstrated by TDCR analysis of the measurement data for the pure ^{14}C source M1 that gave $P = 0.1562$, as opposed to $P = 0.1621$ that was given by the tracer. The differences between the figures-of-merit are likely due to differences in the total amount of radionuclide solution added per source, differences in the chemical compositions of the two radionuclide stock solutions used (Na_2CO_3 in H_2O vs. $NiCl_2$ in HCl), different proportions of the stock solutions used and chemical reactions between Carbo-Sorb and HCl altering chemical quenching. The deviation of P from the value used is expected to decrease as the fraction of ^{14}C in each mixed source decreases and would account for the systematic trend observed in the data (Fig. 3). To assess this effect, the measurement data were analysed with P varying between 0.1562 and 0.1621 according to the mass fraction compositions of the respective sources. This improved the accuracy of the extracted activities for the two sources with the highest ^{14}C contents (M1, M2), but that of the other sources worsened somewhat.

5. Conclusions

A new method for extracting the individual activities from a two-component mixture of pure β-emitters has been demonstrated with the radionuclides ^{63}Ni and ^{14}C. Such combinations of long-lived pure β-emitting radionuclides cannot be determined by following the decay and other available methods rely on calibrated detection systems together with complex spectral analysis or specific window settings.

The present technique offers an alternative elegant solution whereby just two observables, the double- and triple-coincidence rates, together with the experimentally determined figure-of-merit P of the counting system, are sufficient to extract the component activities. It has been shown that reliable results can be obtained over a wide range of compositions, with the accuracy achievable limited only by the accuracy obtainable for P.

References

[1] M.F. L'Annunziata, M.J. Kessler, Liquid scintillation analysis: principles and practice, in: M.F. L'Annunziata (Ed.), Handbook of Radioactivity analysis, second ed, Academic Press, New York, 2003, pp. 418–445.
[2] A. Grau Carles, Appl. Radiat. Isot. 45 (1994) 83.
[3] A. Grau Carles, L. Rodriguez Barquero, A. Grau Malonda, Nucl. Instr. and Meth. A 235 (1993) 234.
[4] T. Altzitzoglou, Appl. Radiat. Isot. 60 (2004) 487.
[5] B.R.S. Simpson, B.R. Meyer, NAC Report NAC/92-02 National Accelerator Centre, Faure, South Africa, 1992.
[6] B.R.S. Simpson, B.R. Meyer, Nucl. Instr. and Meth. A 339 (1994) 14.
[7] A. Grau Malonda, E. García-Toraño, Int. J. Appl. Radiat. Isot. 33 (1982) 249.
[8] B.M. Coursey, A. Grau Malonda, E. García-Toraño, J.M. Los Arcos, Trans. Am. Nucl. Soc. 50 (1985) 13.
[9] E. García-Toraño, A. Grau Malonda, Comp. Phys. Commun. 36 (1985) 307.
[10] Guide to the Expression of Uncertainty in Measurement, first ed., International organization for standardization, Geneva, Switzerland, 1993.
[11] W. Kessel, Termochim. Acta 382 (2002) 1.
[12] M.-M. Bé, B. Duchemin, C. Morillon, E. Browne, V. Chechev, A. Egorov, R. Helmer, E. Schönfeld, Nucleide 2000. Nuclear and atomic decay data, Version 2-2004. BNM-CEA/DTA/LPRI, Saclay, France, 2004.
[13] B.R. Meyer, B.R.S. Simpson, Appl. Radiat. Isot. 41 (1990) 375.
[14] B.R.S. Simpson, W.M. Morris, Appl. Radiat. Isot. 60 (2004) 465.
[15] B.R.S. Simpson, Appl. Radiat. Isot. 56 (2002) 301.